

Observations of canopy flow structure and frictional velocity of coral colonies in DongSha Atoll

Zhi-Cheng Huang, Graduate Inst. of Hydrological and Oceanic Sciences, National Central Univ. Taiwan
Wen-Yang Hsu, Tainan Hydraulics Lab., National Cheng Kung University, Taiwan
Jay Yang, Graduate Inst. of Hydrological and Oceanic Sciences, National Central Univ. Taiwan

INTRODUCTION

Understanding the hydrodynamics is important for biological, ecological, and biogeochemical processes in coral reef systems. The near-bed flow motion affects the benthic organism distributions, morphological evolution, larvae settlement, and nutrient uptake.

The near-bed flow structures have been characterized as planar boundary-layer flows when the bottom roughness scale created by benthic organisms is much smaller than the water depth. On the other hand, when the bottom roughness scale becomes much larger, the resistance drag forces caused by these canopy elements should be considered (Rosman and Hench, 2011). The form drag of the multiple coral colonies generates turbulent wakes, enhances turbulent mixing, and changes the flow structure (Huang, 2015). Many laboratory and modeling studies have reported the drag parameterization and the flow structure for unidirectional flows through submerged canopy or vegetation (e.g., Finnigan, 2000; among many others). However, the vertical flow structures of the canopy layer caused by coral colonies (bommies) are rarely reported in fields.

Here we present field measurements of flow structure over coral colonies using acoustic Doppler velocimetry (ADV) and pulse-coherent Doppler velocity profiler (PCADP) techniques. The measured current profiles and turbulence are used to study the flow dynamics in the canopy-layer created by coral colonies.

EXPERIMENTS

The field experiment was conducted in the northern channel of DongSha atoll (Figure 1) located in the South China Sea (DongSha Atoll Marine National Park, Kaohsiung County; 20.74N, 116.75E) during July 29 - August 28, 2015. The atoll is a circle shape with a diameter of about 25 km. An array of instruments was deployed by scuba divers in a water depth of 5.6 m to measure the waves, currents, and turbulence. Two 5-M



Figure 1. Picture of the study site and the instruments. The red arrow represents the current direction.

Hz ADV-Ocean (ADVO) and one 1.5 MHz PCADP, were up-looking oriented and bottom-mounted on a stainless-steel frame as shown in Figure 1. The instruments were aligned at south-to-north direction to avoid possible wake disturbances by the instruments. The two ADVs were set to measure the 3-D flow velocities for 15600 samples at 16 Hz every 30 minutes at 0.7 and 0.9 m above the seafloor. The PCADP measured the current profiles at a 1 Hz with a 10cm cell size from 0.55 to 2.55 m. The qualities of the measured velocity data were controlled with an outlier removal and interpolation. The measured instantaneous velocity vectors \mathbf{u} were rotated into principle axes of the mean currents.

RESULTS

Figure 2 shows that the recorded data covers two entire spring-neap cycles. The tidal elevation ranged within 1 m during the observational period. The significant wave height H_s was only about 20 cm in days from 210 to 219 with a dominant wave period of about 5 seconds. The wave height varied from 0.5 to 1.2 m and the wave period ranged from about 5 to 18 seconds due to distant swells and energetic wind stress. Considerable infragravity wave components can be seen during days of 219 - 222 and 232 - 237.

The mean current flow and the related water mass flux in Dongsha Atoll affect the biogeochemical and biological status in the atoll lagoon. The current speed measured by PCADP was compared to the upper ADVO as shown in Figure 3a. The good agreement of the result suggests that the PCADP is satisfactory for the detailed current profile measurements. We found

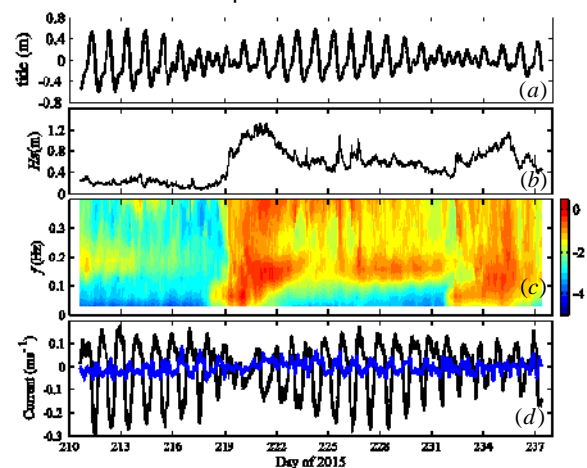


Figure 2. Measured time-series data of (a) tide, (b) significant wave height, (c) spectrogram of waves, and (d) currents (black and blue lines are cross- and along-channel directions as the red arrow in figure 1).

that the tidal current was coming from 148° from the north and it is modulated with the tide (Figure 2 and 3b). The current speed can be respectively up to 0.3 and 0.4 ms^{-1} at 0.9 and 2 m above the bottom. The current are mostly due to major solar the major lunar tidal components as shown in Figure 3c. The observed mean net mass flux is outward the lagoon at the North Channel, implying that the wave-induced driven current along the barrier reef flat of the atoll may provide a positive net flux to bring the water into the lagoon.

Figure 4 illustrates the vertical profiles of the coral-canopy flow structure observed in one spring tidal cycle. The current profiles outside and inside the canopy layer follow logarithmic distributions; however, the slopes of the log-profile vary with some conditions at vertical positions of approximately 1 m that is close to the height of the coral colonies. This can be interpreted as a second log layer due to the form drag caused by the coral bommies. Suppose each velocity profile follows its own law-of-the-wall, the frictional velocities of the two layers can be obtained by fitting the log-profile equation:

$$\begin{aligned} |\bar{u}| &= \frac{|u_{*1}|}{\kappa} \ln\left(\frac{z}{z_{0a1}}\right); \text{ for } z < z_{cp} \\ |\bar{u}| &= \frac{|u_{*2}|}{\kappa} \ln\left(\frac{z}{z_{0a2}}\right); \text{ for } z > z_{cp} \end{aligned} \quad (1)$$

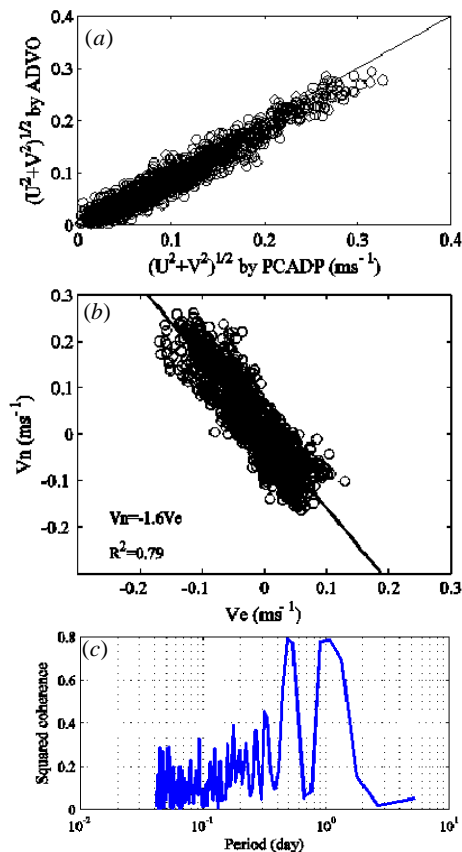


Figure 3. (a) Comparison of the measured current speed by PCADP and ADV0. (b) Scatterplot of the east (V_e) and north (V_n) current components. (c) Squared coherence between tide elevation and current speed.

where u_* is the friction velocity, κ is the von Kármán's constant, and z is the height above the bed, z_{0a} is the apparent hydraulic roughness, and z_{cp} is the inclined point between the two layer. A quality control of R-squared value of the log fit larger than 0.95 is used for the analysis. The variation of the determined frictional velocities for the two logarithmic layers is shown in Figure 5. The slopes of the two log layers show somehow dependence with the current speed though the data are scattered. The hydraulic roughness and frictional velocities also show some dependence with the flood and ebb tidal currents.

The above results highlight that the vertical flow structures of the canopy layer are more complex and a single layer of wall laws and a single hydraulic roughness may be not sufficient to represent the flow structure in coral reefs. More analysis and results of the characteristics of friction velocities coupling with the turbulence statistics of the canopy-layer around coral colonies will be addressed in the conference.

REFERENCES

- Finnigan, J., 2000. Turbulence in plant canopies. *Annu. Rev. Fluid Mech.*, 32, 519-571.
Huang, Z.C., 2015. Vertical structure of turbulence within a depression surrounded by coral-reef colonies. *Coral Reefs*.
Rosman, J.H. and Hench, J.L., 2011. A framework for understanding drag parameterizations for coral reefs. *J. Geophys. Res.*, 116.

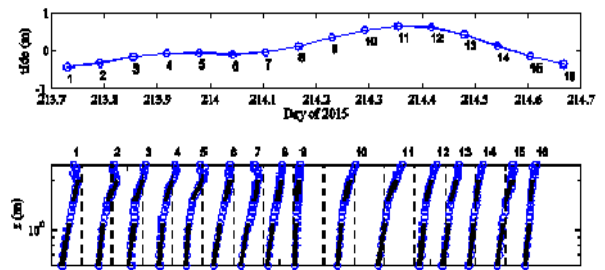


Figure 4. Example of temporal variation of vertical structure of mean currents during a spring tidal cycle. The black lines are the log fits.

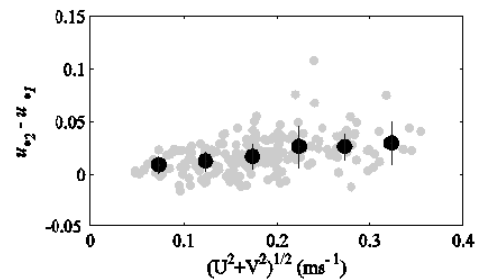


Figure 5. Variation of frictional velocities obtained by fitting two log layers. The presented data are all with $R^2 > 0.95$ for the log fit.